

Reconstructing the general 2HDM charged Higgs boson at the LHC

Wei-Shu Hou[✉] and Mohamed Krab[✉]

Department of Physics, National Taiwan University, Taipei 10617, Taiwan

 (Received 30 May 2024; accepted 4 July 2024; published 30 July 2024)

We study the discovery prospects for a charged Higgs boson via the $bg \rightarrow cH^- \rightarrow c\bar{t}b$ process at the Large Hadron Collider (LHC). Focusing on the general two Higgs doublet model (G2HDM) that possesses extra Yukawa couplings, the process is controlled by extra top couplings ρ_{tc} and ρ_{tt} , which can drive electroweak baryogenesis (EWBG) to account for the baryon asymmetry of the Universe (BAU). We propose benchmark points (BPs) and demonstrate that evidence could emerge at 14 TeV LHC and luminosity of 300 fb^{-1} , with discovery potential at 600 fb^{-1} .

DOI: [10.1103/PhysRevD.110.L011702](https://doi.org/10.1103/PhysRevD.110.L011702)

Introduction. Particle physics is in an *impasse*: other than the $h(125)$ boson that is quite consistent with the Standard Model (SM) Higgs boson, no new physics ($\mathcal{N}\mathcal{N}\mathcal{P}$) has emerged so far! We advocate the general two Higgs doublet model (G2HDM): two identical weak doublets, but allow a second set of Yukawa couplings aside from fermion masses. Though it has not gained much traction, it in fact has quite a few merits.

First, extra top Yukawa couplings $|\rho_{tt}|, |\rho_{tc}| \sim 1$ can each drive [1] electroweak baryogenesis (EWBG), while $\mathcal{O}(1)$ quartic couplings provide [2] the prerequisite 1st order EW phase transition. Second, with CP violation (CPV) $\mathcal{O}(1)$ in strength as is needed for EWBG, one is vulnerable to precision tabletop electron EDM (eEDM) experiments, such as ACME [3] and JILA [4]. However, a spectacular cancellation mechanism was uncovered [5], rooted in the diagrammatics of two-loop diagrams, giving $|\rho_{ee}/\rho_{tt}| \sim \lambda_e/\lambda_t$, where the second ratio is nothing but m_e/m_t . Furthermore, one has a “phase lock,” that $\arg \rho_{ee} = -\arg \rho_{tt}$, to cancel the “ W -loop Higgs- γ - γ^* ” insertion. Could this be the reason behind the “flavor code,” that *Nature setup* fermion mass and mixing hierarchies as observed in SM couplings? Third, the usual criticism [6] of G2HDM is its possession of flavor changing neutral couplings (FCNCs), such as $t \rightarrow ch$ [7]. Interestingly, to date we have not yet observed this plausible decay, as *Nature* seems to throw in small h - H mixing (with H the exotic CP -even boson), $c_\gamma \equiv \cos \gamma$ to control it—*alignment*. *Nature* threw in a purely Higgs-sector parameter *to control FCNC*. Fourth, small c_γ does *not* [8] contradict $\mathcal{O}(1)$

quartics, e.g., η_6 in the second relation of Eq. (2) below. Interestingly, one can then argue that the H, A , and H^\pm bosons *could* populate 300–600 GeV. Finally, with $t \rightarrow ch$ c_γ -suppressed, sub-TeV exotic Higgs masses inspired the $cg \rightarrow tH/tA \rightarrow t\bar{t}, t\bar{t}$ [9] processes, which are unsuppressed by $s_\gamma \equiv \sin \gamma \simeq 1$; these were followed by the more advantageous [10] $cg \rightarrow bH^+ \rightarrow b\bar{t}b$ process, with a recoiling b -jet rather than a heavy top, and receiving Cabibbo-Kobayashi-Maskawa (CKM) enhancement compared to the popular SUSY type 2HDM-II.

We investigate prospects for the H^+ boson in G2HDM to improve H^+ reconstruction compared to $cg \rightarrow bH^+ \rightarrow b\bar{t}b$ [10]. We suggest $pp \rightarrow cH^-$ (plus conjugate) search, which arises from the $bg \rightarrow cH^-$ parton process (Fig. 1), which is again *not* CKM-suppressed. The associated c -jet (\sim “light quark” jet) as tag-jet helps suppress background. We select five BPs that emulate Ref. [10], so $H^+ \rightarrow t\bar{b}$ decay is predominant, and present a signal-to-background analysis at 14 TeV LHC.

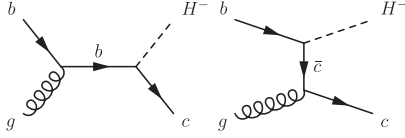
G2HDM.

Higgs couplings: With two identical scalar doublets, in the Higgs basis where only one doublet breaks the symmetry, the most general CP -invariant Higgs potential is [8,11],

$$\begin{aligned}
 V(\Phi, \Phi') = & \mu_{11}^2 |\Phi|^2 + \mu_{22}^2 |\Phi'|^2 - (\mu_{12}^2 \Phi^\dagger \Phi' + \text{H.c.}) \\
 & + \frac{\eta_1}{2} |\Phi|^4 + \frac{\eta_2}{2} |\Phi'|^4 + \eta_3 |\Phi|^2 |\Phi'|^2 + \eta_4 |\Phi^\dagger \Phi'|^2 \\
 & + \left[\frac{\eta_5}{2} (\Phi^\dagger \Phi')^2 + (\eta_6 |\Phi|^2 + \eta_7 |\Phi'|^2) \Phi^\dagger \Phi' \right. \\
 & \left. + \text{H.c.} \right], \tag{1}
 \end{aligned}$$

where η_i 's are quartic couplings and taken as real. Φ generates v to break EW symmetry spontaneously via a

Published by the American Physical Society under the terms of the [Creative Commons Attribution 4.0 International license](https://creativecommons.org/licenses/by/4.0/). Further distribution of this work must maintain attribution to the author(s) and the published article's title, journal citation, and DOI. Funded by SCOAP³.

FIG. 1. Feynman diagrams for the $bg \rightarrow cH^-$ process.

first minimization condition, $\mu_{11}^2 = -\frac{1}{2}\eta_1 v^2$, while $\langle \Phi' \rangle = 0$ hence $\mu_{22}^2 > 0$. A second minimization condition, $\mu_{12}^2 = \frac{1}{2}\eta_6 v^2$, removes μ_{12}^2 as a parameter.

Diagonalizing the h, H mass-squared matrix gives [8,11] mixing angle γ ($\equiv \beta - \alpha$ in 2HDM-II notation),

$$c_\gamma^2 = \frac{\eta_1 v^2 - m_h^2}{m_H^2 - m_h^2}, \quad s_\gamma c_\gamma = \frac{\eta_6 v^2}{m_H^2 - m_h^2}, \quad (2)$$

with approximate alignment implying $c_\gamma \simeq |\eta_6| v^2 / (m_H^2 - m_h^2)$ [8], as s_γ is very close to 1.

The Higgs masses can be written in terms of the potential parameters in Eq. (1),

$$m_{H^+}^2 = \mu_{22}^2 + \frac{1}{2}\eta_3 v^2, \quad m_A^2 = m_{H^+}^2 + \frac{1}{2}(\eta_4 - \eta_5)v^2, \quad (3)$$

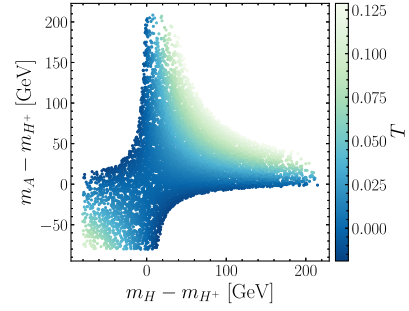
$$m_{H,h}^2 = \frac{1}{2} \left[m_A^2 + (\eta_1 + \eta_5)v^2 \pm \sqrt{(m_A^2 + (\eta_5 - \eta_1)v^2)^2 + 4\eta_6^2 v^4} \right]. \quad (4)$$

The general Yukawa couplings are [11,12]

$$\begin{aligned} \mathcal{L}_Y = & \frac{1}{\sqrt{2}} \sum_{f=u,d,\ell} \bar{f}_i \left[(\lambda_{ij}^f s_\gamma - \rho_{ij}^f c_\gamma) h \right. \\ & - (\lambda_{ij}^f c_\gamma + \rho_{ij}^f s_\gamma) H + i \text{sgn}(Q_f) \rho_{ij}^f A \left. \right] R f_j \\ & - \bar{u}_i [(V \rho^d)_{ij} R - (\rho^{u\bar{t}} V)_{ij} L] d_j H^+ \\ & - \bar{\nu}_i \rho_{ij}^\ell R \ell_j H^+ + \text{H.c.}, \end{aligned} \quad (5)$$

where $i, j = 1, 2, 3$ are generation indices, $L, R = (1 \mp \gamma_5)/2$ and V is the CKM matrix. The elements $\lambda_{ij}^f = \delta_{ij} \sqrt{2} m_i^f / v$ are real with $v \simeq 246$ GeV, while ρ_{ij}^f are non-diagonal and in general complex. Since we assume CP -conserving G2HDM, we shall take ρ_{ij}^f as real in our study. We concentrate on H^\pm production via $bg \rightarrow cH^-$ at the LHC (see Fig. 1), which is governed by the $\bar{c}bH^+$ vertex with coupling $\rho_{tc} V_{tb}$, as can be seen from Eq. (5). We consider $H^+ \rightarrow t\bar{b}$ decay and study the $bg \rightarrow cH^- \rightarrow c\bar{t}b$ signal (plus conjugate) at 14 TeV LHC.

Constraints on parameter space: The parameter space is subject to various constraints. On theory side, we demand all

FIG. 2. Scan points for possible mass separation between H^+ , H , and A bosons. The color bar represents the T parameter.

parameters in Eq. (1) to satisfy vacuum stability, tree-level unitarity and perturbativity, which are checked using the program 2HDMC-1.8.0 [13]. As η_1, η_{3-6} appear in exotic Higgs masses [Eqs. (3) and (4)], we first express these quartic couplings in terms of $m_{h,H,A,H^+}^2, \mu_{22}^2, \gamma$, and v [11], then randomly scan over $m_{H^+}, m_A, m_H, \mu_{22}^2, \eta_2, \eta_7$ within following ranges: $m_{H^+} \in [300, 600]$ GeV, $m_{H,A} \in [m_{H^+} - m_W, 650]$ GeV, $\mu_{22}^2 \in [0, 10^6]$ GeV², $|\eta_{2,7}| \leq 3$ (this $\mathcal{O}(1)$ condition is imposed on all η_i s). We fix $m_h = 125$ GeV and set $c_\gamma = 0$, as H^+ couplings do not depend on c_γ . Thus, $\eta_1 = m_h^2 / v^2 \simeq 0.258$ and $\eta_6 = 0$.

The scan is done via 2HDMC, which employs Λ_{1-7} and m_{H^+} as Higgs basis inputs. We define η_{1-7} as Λ_{1-7} , and require parameters to satisfy EW precision S, T, U [14] parameter constraints, with PDG fits (for $U = 0$) [15]: $S = 0.05 \pm 0.08$ and $T = 0.09 \pm 0.07$, with correlations taken into account.

The parameters satisfying theory and EW precision constraints (at 2σ level) are plotted in the $(m_H - m_{H^+}, m_A - m_{H^+})$ plane, as shown in Fig. 2. The color code depicts the size of T parameter, which constrains the masses of H, A, H^+ . We see that m_{H^+} remains close to m_H and/or m_A . Since we focus on $H^+ \rightarrow t\bar{b}$ decays as motivated by existing experimental H^+ searches, we assume the mass hierarchy $m_{H^+} \sim m_H$ and/or $m_{H^+} \sim m_A$. Thus, $H^+ \rightarrow W^+ H$ and/or $H^+ \rightarrow W^+ A$ decays are kinematically inaccessible (see Ref. [16] for implications of $H^+ \rightarrow W^+ A$ in G2HDM).

We illustrate with five benchmarks, with $m_{H^+} = 300\text{--}500$ GeV in 50 GeV steps, as listed in Table I. Note that BP1 and BP5 are BP1 and BP2 of Ref. [10].

There are experimental limits from flavor and collider physics. For simplicity, we set all $\rho_{ij} = 0$ other than the involved ρ_{tc}, ρ_{tt} couplings. Flavor constraints are not stringent [17,18]. The constraints from $B_s\text{--}\bar{B}_s$ mixing and $b \rightarrow s\gamma$ on ρ_{tc} are weak due to small m_c [18]. It was found that $|e_{32}^u| \geq 1.3(1.7)$ is excluded by $B_s\text{--}\bar{B}_s$ mixing for $m_{H^+} = 300(500)$ GeV and $\tan\beta = 50$. This leads to the bound $|\rho_{tc}| \lesssim 1.3(1.7)$ for $m_{H^\pm} = 300(500)$ GeV. For detailed discussion, see Ref. [18].

The observables $B_q\text{--}\bar{B}_q$ ($q = s, d$) and $b \rightarrow s\gamma$ also put constraints on ρ_{tt} and ρ_{ct} . The latter is strongly constrained

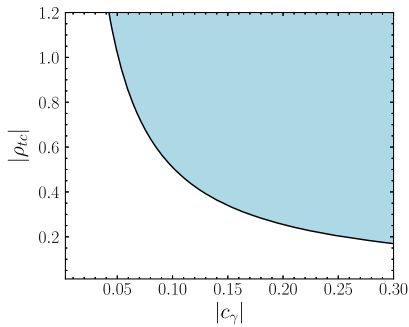
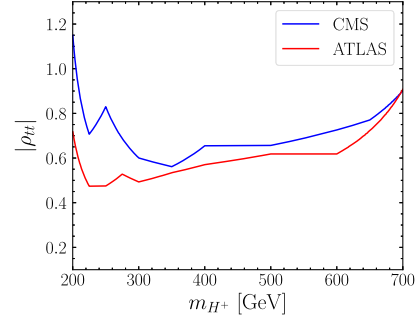
TABLE I. Benchmark parameters for BP1-BP5. All masses in GeV, with $\eta_6 = 0$, $m_h = 125$ GeV for all BPs.

BP	η_2	η_3	η_4	η_5	η_7	m_{H^+}	m_A	m_H	μ_{22}^2/v^2
1	1.40	0.62	0.53	1.06	-0.79	300	272	372	1.18
2	0.93	1.06	0.14	-0.36	-0.22	350	371	340	1.49
3	1.36	1.16	0.81	0.70	-0.36	400	404	454	2.06
4	0.61	1.83	1.30	-0.30	0.68	450	501	482	2.46
5	0.71	0.69	1.52	-0.93	0.24	500	569	517	3.78

by $B_q-\bar{B}_q$ due to enhanced CKM factor $|V_{cq}/V_{tq}| \sim 25$, hence ρ_{ct} must be tiny [17]. Regardless of ρ_{ct} , the limit on ρ_{tt} is rather weak, leading to the upper bound $|\rho_{tt}| \lesssim 1.2(1.5)$, however, for $\rho_{ct} \lesssim 0.05(0.06)$, $0.5 \lesssim |\rho_{tt}| \lesssim 1.2(1.5)$ for $m_{H^+} = 300(500)$ GeV [17]. Therefore, ρ_{ct} is turned off. Because of a m_t/m_b enhancement factor, the limit from $b \rightarrow s\gamma$ constrains ρ_{bb} more severely than ρ_{tt} , hence ρ_{bb} is turned off. More details can be found in Ref. [17]. Note that the selected benchmarks, $\rho_{tc}, \rho_{tt} = 0.4, 0.6$, satisfy both constraints from $B_q-\bar{B}_q$ mixing and $b \rightarrow s\gamma$.

The ρ_{tc}, ρ_{tt} couplings are further constrained by collider data. For $c_\gamma \neq 0$, $t \rightarrow ch$ searches set significant constraint on ρ_{tc} , where both CMS [19] and ATLAS [20,21] set 95% CL limits with full Run 2 data. We illustrate the most stringent ATLAS limit [21] and find $|\rho_{tc}| \gtrsim 0.5$ is excluded at 95% CL for $c_\gamma = 0.1$ (see Fig. 3). The limit shrinks with c_γ and disappears in alignment limit. The ρ_{tc} parameter receives further stringent constraint from CMS four top search [22]. See Refs. [16,23,24] for more discussion.

ATLAS [25] and CMS [26] direct searches for $H^+ \rightarrow t\bar{b}$ at LHC strongly constrain ρ_{tt} . ATLAS uses full 139 fb⁻¹ Run 2 data, while CMS used only 35.9 fb⁻¹ so far, hence the ATLAS limit is more stringent on $\sigma(pp \rightarrow \bar{t}bH^+) \cdot \mathcal{B}(H^+ \rightarrow t\bar{b})$ for m_{H^+} between 0.2 and 2 TeV. We illustrate these limits assuming $\mathcal{B}(H^+ \rightarrow t\bar{b}) = 100\%$ to constrain ρ_{tt} with leading order (LO) cross section estimates with MadGraph5_aMC@NLO [27], using the 2HDM model file in Ref. [28], and K -factor ~ 1.6 [29] to account for NLO corrections, as illustrated in Fig. 4; the CMS bounds are also depicted for comparison. LHC searches for


 FIG. 3. ATLAS $t \rightarrow ch$ exclusion limit [21] in $|c_\gamma|$ - $|\rho_{tc}|$ plane.

 FIG. 4. Exclusion bounds from ATLAS [25] and CMS [26] searches for $pp \rightarrow \bar{t}bH^+ \rightarrow \bar{t}bt\bar{b}$ in the m_{H^+} - $|\rho_{tt}|$ plane.

$pp \rightarrow H/A \rightarrow t\bar{t}$ [30,31] and $pp \rightarrow ttH/A \rightarrow t\bar{t}\bar{t}$ [22] also constrain ρ_{tt} , but these constraints are slightly weaker than direct H^+ searches and $B_{d,s}$ mixing [10]. Direct and indirect LHC measurements can put further bounds on ρ_{tt} (also c_γ [32]), specifically $t\bar{t}h$ and Higgs property measurements. These bounds suffer c_γ suppression, however, as seen from Eq. (5). Note that our chosen ρ_{tt} is safe from all constraints mentioned.

Collider study. We study H^- production in association with a c quark, $bg \rightarrow cH^-$ (see Fig. 1). With $H^- \rightarrow \bar{t}b$ decay for all BPs, the signal would have three jets, at least two identified as b -jets, plus one lepton and missing transverse momentum. With this novel signature, a b -jet and the lepton plus neutrino can be used to reconstruct a top, then combine with the other b -jet to reconstruct the H^+ . But for the $bt\bar{b}$ signature of Ref. [10] with three b -jets (or even worse for $\bar{t}bH^+ \rightarrow \bar{t}bt\bar{b}$), the high b -jet multiplicity makes H^+ reconstruction more difficult. Our final state has a further high p_T “tag”-jet. Thus, our signature is complementary to existing direct searches for H^+ .

We follow the $cg \rightarrow \bar{b}H^+ \rightarrow bt\bar{b}$ analysis of Ref. [10], which has one extra b -tagged jet.¹ The analysis was extended further to improve sensitivity [33].

For the BPs listed in Table I, for $\rho_{tc} = 0.4, \rho_{tt} = 0.6$, the $\mathcal{B}(H^+ \rightarrow c\bar{b}), \mathcal{B}(H^+ \rightarrow t\bar{b})$ values are 50% (44%, 40%, 38%, 36%) and 50% (56%, 60%, 62%, 64%) for BP1 (BP2, BP3, BP4, BP5), respectively.² Considering the $bg \rightarrow cH^- \rightarrow c\bar{t}b$ signal, assuming $t \rightarrow \ell (e \text{ or } \mu) + \nu + b$ -jet decay, the final state should be two b -jets, one high p_T jet, plus one lepton and missing E_T from ν . The subdominant $bg \rightarrow tH^- \rightarrow t\bar{c}b$ is also included as signal. The main background is SM $t\bar{t}$ production in association with flavor jets. Other backgrounds are single top (tj), $Wt + \text{jets}$, $t\bar{t}h$, and $t\bar{t}Z$. Drell-Yan, $W + \text{jets}$, $t\bar{t}W$, and tWh backgrounds are minor.

¹Our signal is included as subdominant contribution to the one proposed in Ref. [10], but killed by applied cuts.

² $H^+ \rightarrow c\bar{b}$ decay dominates at low m_{H^+} , especially below m_t , where the $H^+ \rightarrow t\bar{b}$ decay is kinematically forbidden.

TABLE II. Cross sections (fb) at 14 TeV after selection cuts.

BP	$t\bar{t} + 2j$	$Wt + 2j$	$tj + 1j$	$t\bar{t}h$	$t\bar{t}Z$	Signal
1	3143.2	699.2	228.1	1.5	0.9	14.9
2	2237.9	548.3	185.8	1.4	0.8	11.9
3	2782.1	816.5	222.5	1.9	1.1	13.8
4	2438.2	752.2	157.5	2.0	1.4	9.8
5	1894.8	605.5	108.1	1.7	1.0	6.4

Signal and background cross sections are computed at LO using MadGraph5_aMC@NLO with default NN23LO1 PDF at 14 TeV collision energy. All samples are passed through Pythia8 [34] for parton showering and hadronization, then processed through fast detector simulator DELPHES [35] with ATLAS card and anti-kt jet algorithm [36], and with $\Delta R = 0.5$. The resulting signal and background events are analyzed using MadAnalysis5 [37]. Backgrounds are rescaled using K -factors to account for NLO (or higher) QCD corrections. The K -factors for $t\bar{t} + \text{jets}$, $Wt + \text{jets}$, $t(s)$ -channel single top, $t\bar{t}h$ and $t\bar{t}Z$ processes are 1.84 [38], 1.35 [39], 1.2 (1.47) [40], 1.27 [41], and 1.56 [42], respectively. Signal cross sections are kept at LO.

Candidate signal events are with at least two jets and no more than four jets, at least two b -tagged with $p_T^j > 20$ GeV, plus one lepton with $p_T^\ell > 30$ GeV, and $E_T^{\text{miss}} > 20$ GeV. The angular separation ΔR between all jet-pairs, and any jet plus lepton should be larger than 0.4. The pseudo-rapidity $|\eta|$ of lepton and all jets should satisfy $|\eta| < 2.5$. The H_T sum of lepton, leading jet and two b -jets should be larger than 350 (400) GeV for BP1 (BP2-5). To further reduce backgrounds, especially $t\bar{t} + \text{jets}$, $Wt + \text{jets}$ and tj contributions, the transverse mass of reconstructed H^+ should lie within $m_{H^+} \pm 50$ GeV mass window. We give the background and signal cross sections in Table II for each BP.

We estimate our signal sensitivity using $\mathcal{Z} = \sqrt{2[(S+B)\ln(1+S/B) - S]}$ [43] for statistical significance, where S is number of signal events and B for background events. We find significance for BP1 (BP2, BP3) $\simeq 4.0\sigma$ (3.8σ , 3.9σ) at 300 fb^{-1} , and $\simeq 5.7\sigma$ (5.3σ , 5.5σ) at 600 fb^{-1} . With 140 fb^{-1} , one has $\sim 2.8\sigma$ (2.6σ , 2.6σ) significance for BP1 (BP2, BP3). Thus, evidence (hint) could emerge with 300 (140) fb^{-1} data, while 600 fb^{-1} could claim discovery. With $m_{H^+} = 400$ GeV (BP3) and $L = 300 \text{ fb}^{-1}$, $\rho_{tc} = 0.3$ and $\rho_{tt} = 0.4$ can give $\mathcal{Z} \simeq 2.0\sigma$, while larger values could yield $\mathcal{Z} \sim 5\sigma$ or higher (see Fig. 5). For BP4 and BP5, we find $\simeq 2.9\sigma$ (4.1) and $\sim 2.2\sigma$ (3.1σ) at 300 fb^{-1} (600 fb^{-1}), respectively. The significance at 140 fb^{-1} is $\simeq 2.0\sigma$ for BP4 and less than 2σ for BP5. For these BPs, evidence (hint) should emerge at 600 (300) fb^{-1} . Note that the significance for $cg \rightarrow bH^+ \rightarrow b\bar{t}$ is $\simeq 4.9$ (5.0) and $\simeq 6.9$ (7.1) for BP1 (BP5) at 300 and 600 fb^{-1} , respectively [10].

Before closing, we note the ρ_{tu} coupling can induce $bg \rightarrow uH^- \rightarrow ut\bar{b}$, but ρ_{tu} is highly constrained. For

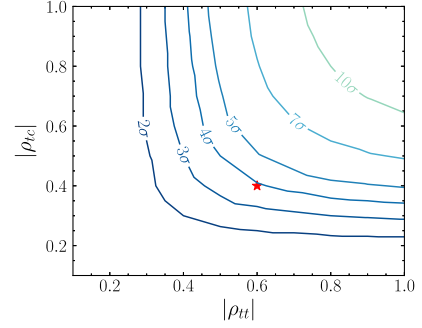


FIG. 5. Significance in the $|\rho_{tt}|$ - $|\rho_{tc}|$ plane. BP3, which corresponds to a significance of $\sim 3.9\sigma$, is shown as a red star.

$\rho_{tt} = 0.6$, it was found that [10] with all other $\rho_{ij} = 0$, $|\rho_{tu}| \gtrsim 0.1$ (0.2) is excluded at 95% CL by CRW of Ref. [22] for BP1 (BP5). For instance, taking $\rho_{tu} = 0.1$ and $\rho_{tt} = 0.6$ (setting $\rho_{tc} = 0$), $\mathcal{B}(H^+ \rightarrow u\bar{b})$ and $\mathcal{B}(H^+ \rightarrow t\bar{b})$ are 6% and 94%, respectively. The achievable significance for BP1 is less than 1σ even for 600 fb^{-1} . We therefore neglect the ρ_{tu} contribution in our study.

In addition, the presence of other ρ_{ij} s, e.g. $\rho_{\tau\tau}$ would induce $H^+ \rightarrow \tau^+\nu_\tau$ decay, which can dilute $\mathcal{B}(H^+ \rightarrow t\bar{b})$ hence the signal. Taking $\rho_{\tau\tau} \sim \lambda_\tau$, however, would not change our conclusions because $\mathcal{B}(H^+ \rightarrow \tau^+\nu_\tau)$ is tiny. Non-zero ρ_{bb} induces $H^+ \rightarrow t\bar{b}$ decay and hence can yield $\bar{c}H^+$ signature. But for $\rho_{bb} \sim \lambda_b$, the contribution is negligible compared to $\rho_{tt} \sim 0.6$.

Discussion and summary. Searches for H^+ boson with mass above m_t (typically called ‘‘heavy’’ H^+) have relied on associated production with a top and bottom quark in the 4-flavor scheme, $pp \rightarrow \bar{t}bH^+$, and with top quark in the 5-flavor scheme, $pp \rightarrow \bar{t}H^+$. These processes were mostly motivated by MSSM (and 2HDM-II). In G2HDM, the novel $pp \rightarrow bH^+$ process (dominated by cg -initiated channel due to $\rho_{tc}V_{tb}$ coupling) was proposed [10]. Assuming $H^+ \rightarrow t\bar{b}$ decay, it would yield a signature with at least three b -jets, one lepton and missing p_T . The high b -jet multiplicity makes it relatively difficult to reconstruct H^+ .

We propose a search for a charged Higgs boson in association with a light quark jet, with production cross section larger than typical H^+ production in association with a top quark, with $H^+ \rightarrow t\bar{b}$ decay. This novel signal would have two b -jets, one extra jet plus one lepton and missing E_T . It would be useful to probe H^+ further at the LHC with this alternative signature, especially if one sees a hint in $pp \rightarrow bH^+ \rightarrow b\bar{t}$. The proposed signal can be useful to discriminate G2HDM from other two Higgs doublet extensions, such as 2HDM-II, where the $bg \rightarrow cH^-$ process is CKM suppressed.

The presence of the FCNC coupling ρ_{tc} has significant impact on the Z_2 forbidden tree-level Higgs production

process like $pp \rightarrow tH/A$ [9,44] (as well as controlling V_{tb} proportional $pp \rightarrow H^+ \bar{c}/b$ processes) and decay channels like $t \rightarrow ch$ [7], and $H/A \rightarrow t\bar{c}$ [44]. These provide substantial avenues to complement existing direct and indirect LHC searches for exotic Higgs bosons (also at low energy). Moreover, ρ_{tc} can drive electroweak baryogenesis in case ρ_{tt} becomes ineffective [1,5]. Thus, ρ_{tc} can crucially open the door for more intriguing new physics scenarios. Observing those induced ρ_{tc} processes would be a smoking gun for G2HDM.

In summary, we investigate the discovery prospect for a charged Higgs boson through the $bg \rightarrow qH^- \rightarrow q\bar{t}b$ process. We present five BPs, with H^+ masses ranging from 300 to 500 GeV, and did a signal-to-background study. We find evidence could emerge with 300 fb^{-1} at 14 TeV collision, and possible discovery at 600 fb^{-1} .

Acknowledgments. This work is supported by NSTC Grant No. 112-2639-M-002-006-ASP of Taiwan, and NTU Grants No. 113L86001 and No. 113L891801.

-
- [1] K. Fuyuto, W.-S. Hou, and E. Senaha, *Phys. Lett. B* **776**, 402 (2018).
- [2] S. Kanemura, Y. Okada, and E. Senaha, *Phys. Lett. B* **606**, 361 (2005).
- [3] V. Andreev *et al.* (ACME Collaboration), *Nature (London)* **562**, 355 (2018).
- [4] T. S. Roussy *et al.*, *Science* **381**, 46 (2023).
- [5] K. Fuyuto, W.-S. Hou, and E. Senaha, *Phys. Rev. D* **101**, 011901(R) (2020).
- [6] S. L. Glashow and S. Weinberg, *Phys. Rev. D* **15**, 1958 (1977).
- [7] W.-S. Hou, *Phys. Lett. B* **296**, 179 (1992).
- [8] W.-S. Hou and M. Kikuchi, *Europhys. Lett.* **123**, 11001 (2018).
- [9] M. Kohda, T. Modak, and W.-S. Hou, *Phys. Lett. B* **776**, 379 (2018).
- [10] D. K. Ghosh, W.-S. Hou, and T. Modak, Companion Letter, *Phys. Rev. Lett.* **125**, 221801 (2020).
- [11] S. Davidson and H. E. Haber, *Phys. Rev. D* **72**, 035004 (2005).
- [12] W.-S. Hou and T. Modak, *Phys. Rev. D* **101**, 035007 (2020).
- [13] D. Eriksson, J. Rathsmann, and O. Stål, *Comput. Phys. Commun.* **181**, 189 (2010).
- [14] M. E. Peskin and T. Takeuchi, *Phys. Rev. D* **46**, 381 (1992).
- [15] P. A. Zyla *et al.* (Particle Data Group), *Prog. Theor. Exp. Phys.* **2020**, 083C01 (2020).
- [16] W.-S. Hou and T. Modak, *Phys. Rev. D* **103**, 075015 (2021).
- [17] B. Altunkaynak, W.-S. Hou, C. Kao, M. Kohda, and B. McCoy, *Phys. Lett. B* **751**, 135 (2015).
- [18] A. Crivellin, C. Greub, and A. Kokulu, *Phys. Rev. D* **87**, 094031 (2013).
- [19] A. Tumasyan *et al.* (CMS Collaboration), *Phys. Rev. Lett.* **129**, 032001 (2022).
- [20] G. Aad *et al.* (ATLAS Collaboration), *J. High Energy Phys.* **12** (2023) 195.
- [21] G. Aad *et al.* (ATLAS Collaboration), arXiv:2404.02123.
- [22] A. M. Sirunyan *et al.* (CMS Collaboration), *Eur. Phys. J. C* **80**, 75 (2020).
- [23] W.-S. Hou, M. Kohda, and T. Modak, *Phys. Lett. B* **798**, 134953 (2019).
- [24] W.-S. Hou and T. Modak, *Mod. Phys. Lett. A* **36**, 2130006 (2021).
- [25] G. Aad *et al.* (ATLAS Collaboration), *J. High Energy Phys.* **06** (2021) 145.
- [26] A. M. Sirunyan *et al.* (CMS Collaboration), *J. High Energy Phys.* **07** (2020) 126.
- [27] J. Alwall, R. Frederix, S. Frixione, V. Hirschi, F. Maltoni, O. Mattelaer, H.-S. Shao, T. Stelzer, P. Torrielli, and M. Zaro, *J. High Energy Phys.* **07** (2014) 079.
- [28] C. Degrande, *Comput. Phys. Commun.* **197**, 239 (2015).
- [29] C. Degrande, R. Frederix, V. Hirschi, M. Ubiali, M. Wiesemann, and M. Zaro, *Phys. Lett. B* **772**, 87 (2017).
- [30] M. Aaboud *et al.* (ATLAS Collaboration), *Phys. Rev. Lett.* **119**, 191803 (2017).
- [31] A. M. Sirunyan *et al.* (CMS Collaboration), *J. High Energy Phys.* **04** (2020) 171.
- [32] W.-S. Hou, M. Kohda, and T. Modak, *Phys. Rev. D* **98**, 075007 (2018).
- [33] N. Desai, A. Mariotti, M. Tabet, and R. Ziegler, *J. High Energy Phys.* **11** (2022) 112.
- [34] T. Sjöstrand, S. Ask, J. R. Christiansen, R. Corke, N. Desai, P. Ilten, S. Mrenna, S. Prestel, C. O. Rasmussen, and P. Z. Skands, *Comput. Phys. Commun.* **191**, 159 (2015).
- [35] J. de Favereau, C. Delaere, P. Demin, A. Giammanco, V. Lemaître, A. Mertens, and M. Selvaggi (DELPHES 3 Collaboration), *J. High Energy Phys.* **02** (2014) 057.
- [36] M. Cacciari, G. P. Salam, and G. Soyez, *J. High Energy Phys.* **04** (2008) 063.
- [37] E. Conte, B. Fuks, and G. Serret, *Comput. Phys. Commun.* **184**, 222 (2013).
- [38] <https://twiki.cern.ch/twiki/bin/view/LHCPhysics/TtbarNNLO>.
- [39] N. Kidonakis, *Phys. Rev. D* **82**, 054018 (2010).
- [40] <https://twiki.cern.ch/twiki/bin/view/LHCPhysics/SingleTopRefXsec>.
- [41] <https://twiki.cern.ch/twiki/bin/view/LHCPhysics/CERNYellowReportPageAt14TeV2010>.
- [42] J. Campbell, R. K. Ellis, and R. Röntsch, *Phys. Rev. D* **87**, 114006 (2013).
- [43] G. Cowan, K. Cranmer, E. Gross, and O. Vitells, *Eur. Phys. J. C* **71**, 1554 (2011).
- [44] W.-S. Hou, M. Kohda, and T. Modak, *Phys. Lett. B* **786**, 212 (2018).